

Pockmarks and seafloor instability in the Olbia continental slope (northeastern Sardinian margin, Tyrrhenian Sea)

Giacomo Dalla Valle · Fabiano Gamberi

Received: 27 July 2010 / Accepted: 7 April 2011 / Published online: 7 July 2011
© Springer Science+Business Media B.V. 2011

Abstract The seafloor morphology and the subsurface of the continental slope of the Olbia intraslope basin located along the eastern, passive Sardinian margin (Tyrrhenian Sea) has been mapped through the interpretation of high-resolution multibeam bathymetric data, coupled with air-gun and sparker seismic profiles. Two areas, corresponding to different physiographic domains, have been recognized along the Olbia continental slope. The upper slope domain, extending from 500 to 850 m water depth, exhibits a series of conical depressions, interpreted as pockmarks that are particularly frequent in seafloor sectors coincident with buried slope channels. In one case, they are aligned along a linear gully most likely reflecting the course of one of the abandoned channels. The location of the pockmarks thus highlights the importance of the distribution of lithologies within different sedimentary bodies in the subsurface in controlling fluid migration plumbing systems. A linear train of pockmarks is, however, present also away from the buried channels being related to a basement step, linked to a blind fault. Two bathymetric highs, interpreted as possible carbonate mounds, are found in connection with some of the pockmark fields. Although the genetic linkage of the carbonate mounds with seafloor fluid venting cannot be definitively substantiated by the lack of in situ measurements, the possibility of a close relationship is here proposed. The lower slope domain, from 850 m down to the base of the slope at 1,200 m water depth is characterized by a sudden gradient increase (from 2° to 6°) that is driven by the presence of the basin master fault that separates the continental slope from the basin plain. Here, a series of

km-wide headwall scars due to mass wasting processes are evident. The landslides are characterized by rotated, relatively undeformed seismic strata, which sometimes evolve upslope into shallow-seated (less than 10 m), smaller scale failures and into headless chutes. Slope gradient may act as a major controlling factor on the seafloor instability along the Olbia continental slope; however, the association of landslides with pockmarks has been recognized in several continental slopes worldwide, thus the role of over-pressured fluids in triggering sediment failure in the Olbia slope can not be discarded. In the absence of direct ground truthing, the geological processes linked to subsurface structures and their seafloor expressions have been inferred through the comparison with similar settings where the interpretation of seafloor features from multibeam data has been substantiated with seafloor sampling and geochemical data.

Keywords Pockmark · Submarine channel · Carbonate mound · Submarine landslide · Multibeam · Seafloor morphology · Eastern Sardinian margin

Introduction

In recent years, our understanding of geological processes acting on submarine slopes has greatly advanced through the interpretation of both modern and ancient systems (Pratson et al. 1996; Weimer and Slatt 2004; Flint and Hodgson 2005 and references therein). In particular, the complex seafloor morphology and subsurface setting of modern continental slopes has been revealed through the coupling of high resolution multibeam echo-sounders and side-scan sonar equipment with 2D and 3D seismic data (Locat et al. 1999; Dugan and Flemings 2000; Posamentier

G. Dalla Valle (✉) · F. Gamberi
Istituto di Scienze Marine (ISMAR-Geologia Marina), CNR,
via Gobetti 101, 40129 Bologna, Italy
e-mail: giacomo.dalla.valle@bo.ismar.cnr.it

and Kolla 2003; Steffens et al. 2004; Mosher and Piper 2007; Normark et al. 2009). In particular, geophysical and geochemical investigations of the seabed have provided striking evidence for the widespread seepage of gas-rich fluid at the seafloor in different sedimentary environments along continental margins, both in active and passive settings (Judd and Hovland 2007 and references therein). The study of the processes associated with subsurface fluid migration have received increasing attention because they give information regarding the distribution of hydrocarbons in the subsurface, and the degree of integrity of the reservoirs (O'Brien et al. 2002; Heggland 2005; Ligtenberg 2005; Van Rensbergen et al. 2007). Fluid venting at the seafloor also plays a crucial role in the establishment of specific and unexpected ecosystems at the seafloor, and furthermore, it can represent a substantial hazard to exploration drilling and to offshore installations (Sultan et al. 2001; Hovland et al. 2002; Judd and Hovland 2007; Pilcher and Argent 2007; Zakeri 2009; Cathles et al. 2010).

Along continental margins, many slope sectors show a close relationship between sedimentary dynamics, subseafloor stratigraphy, structural setting, subsurface fluid migration pathways and seafloor seepage (Boe and Ottesen 1998, Gay et al. 2006). Seafloor conical depressions, formed as a consequence of fluid expulsion (pockmarks; King and MacLean 1970), occur in many submarine slopes worldwide (Hovland 1991; Rise et al. 1999; Cochonat et al. 2002; Berndt 2005; Rollet et al. 2006; Gay et al. 2007). Recently, pockmarks have also been observed on seafloor sectors marking the courses of shallowly buried channels (Gay et al. 2003, 2006) or in correspondence with deep and shallow tectonic or salt-related structures (Geletti et al. 2008; Andersen and Huuse 2011). Complexes of pockmarks are also found in association with authigenic carbonate ridges and carbonate mounds, especially in the Atlantic margin of Europe and in the Mediterranean Sea (Aloisi et al. 2000; Magalhães et al. 2003; Hovland et al. 2005; Masson et al. 2003; Mazzini et al. 2004; Dupré et al. 2007; Judd et al. 2007; Bayon et al. 2009a, b; Huguen et al. 2009; Dupré et al. 2010). It has been documented that gas and fluids entrapped in the subsurface can lower the shear strength of the sediment, triggering in turn submarine landslides (Kvalstad et al. 2005; Paull et al. 2007). Also active or inherited tectonic structures can promote and enhance landslides, by controlling the slope topography and the gradient and the distribution of subsurface discontinuities that can also be used by fluids as preferential escape pathways (Gay et al. 2007; Géli et al. 2008; Xie et al. 2003; Hovland et al. 2010; Huuse et al. 2010). In terms of geohazard assessment, gas seepage is an element to be carefully considered, and the recognition of the geomorphic elements directly linked to it is crucial in terms of risk assessment and mitigation.

In this work, through the analysis of high-resolution multibeam bathymetric data and seismic profiles, we present a morphological description of the seafloor and shallow subsurface of the Olbia continental slope (eastern Sardinian margin). The main aim of this work is to map the geomorphology and the internal geometries of the features linked to subsurface and seafloor fluid flow and to sediment instability that can represent a potential geohazard for offshore installations and the environment. In the study area, geotechnical and geochemical seafloor samples are not available, thus the activity of the geological features linked to fluid venting (pockmarks and carbonate mud mounds) are not directly assessed. Notwithstanding, we propose an interpretation where features and processes related to geohazards have been reconstructed through the coupling of multibeam and shallow subsurface data. Further studies through direct in situ investigations are however necessary to verify the present-day activity of these geological processes along the Olbia continental slope.

Regional setting

The eastern Sardinian margin is the passive margin of the central Tyrrhenian back-arc basin, formed as a consequence of the European-African collision (Malinverno and Ryan 1986) (Fig. 1). In the Sardinian sector, rifting started in the Late Miocene (Tortonian) and ended in the Late Pliocene (Kastens and Mascle 1990; Sartori 1990). Along the eastern Sardinian margin, the rifting morphology is still evident as a series of structural highs that bound the intraslope basins of the upper sector of the margin. The continental slope of the Olbia intraslope basin, the subject of this study, is located in the northern part of the eastern Sardinian margin (Fig. 1). The slope is around 25 km wide (Figs. 1, 2a) and is flanked landward by a 20 km wide shelf, with the shelf-break located at around 120 m water depth (Ulzega et al. 1988).

Seismic profiles show that the continental slope is characterized by a marked high-amplitude reflector corresponding to the Messinian unconformity (Fabbri and Curzi 1979). A seismic profile crossing the DSDP Site 132 (in the center of the Tyrrhenian basin) shows that this interval coincides with the top of the evaporite sequence and that it is probably composed of horizons of sulphate evaporites that alternate with terrigenous sediments (Ryan et al. 1973). In the Olbia continental slope, the seismic profiles show that the Messinian reflector lies below around 0.20 s of Plio-Quaternary deposits, thus indicating a low rate of sedimentation (averaging ~ 3.37 cm/1,000 years). Morphologically, the Olbia continental slope is composed of an upper, low gradient, less than 2° dipping sector (from 500 to 850 m depth), and a lower (downslope from 850 m to

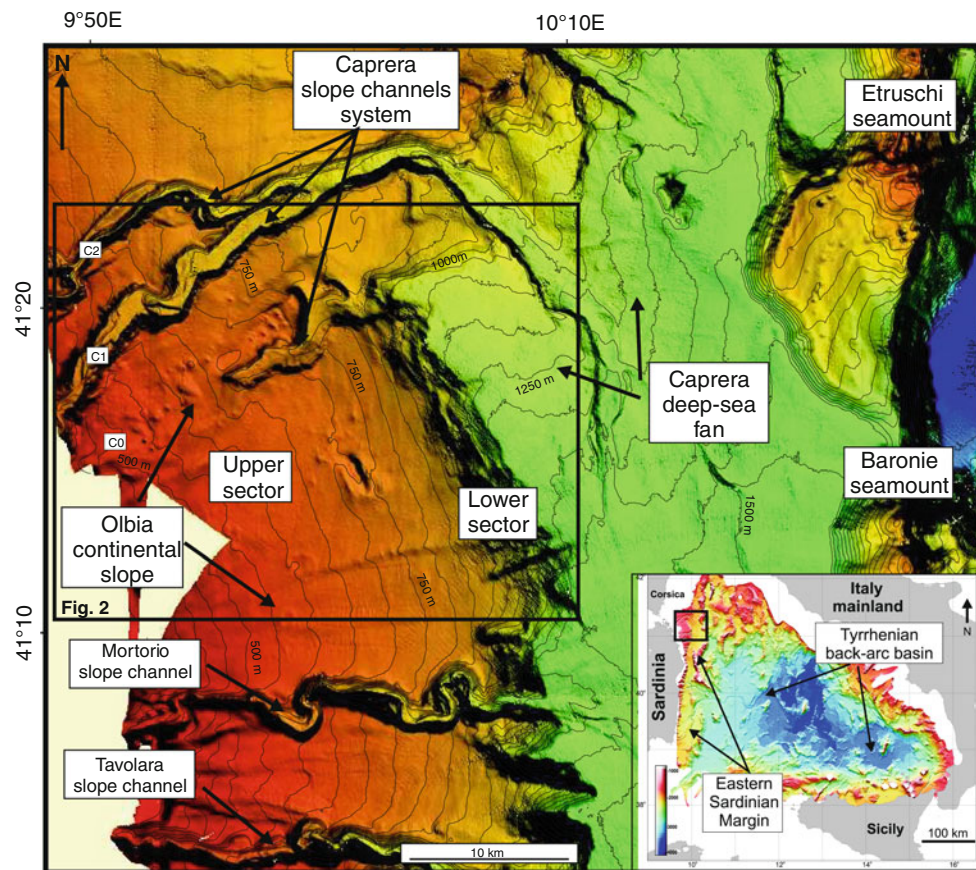


Fig. 1 Shaded relief map of the northern sector of the Olbia intraslope basin in the Tyrrhenian Sea from multibeam bathymetric data (see location in the *lower right inset*). The Olbia intraslope basin is articulated in a 25 km wide continental slope, a 20 km wide basin plain that is bordered to the east by the Etruschi and Baronie seamounts. The study area corresponds with the *box* and is shown in

more detail in Fig. 2 The studied sector of the Olbia continental slope is bordered to the north by the *C1* and *C2* slope channels and to the south by the Mortorio slope channel. The southernmost slope channel systems of the Olbia basin, the Tavolara system, is also indicated. Contour interval: 50 m

around 1,250 m), high gradient, 6° dipping sector (Figs. 1, 2a) controlled by a high-angle extensional fault that separates the continental slope from the Olbia basin (Marani et al. 2004; Gamberi and Dalla Valle 2009; Dalla Valle and Gamberi 2010). Owing to the lack of seismicity along the eastern Sardinian margin, the fault is considered, at the present, to be an inactive tectonic element (Marani et al. 2004). The Olbia continental slope is dissected by several slope channel systems, of which the main is the Caprera system that consists of three distinct slope channels (Figs. 1, 2a). Two of these channels (*C1* and *C2*) are considered still active (Dalla Valle and Gamberi 2010), whereas the southernmost channel (*C0*) is almost completely abandoned (Figs. 1, 2a). At present, the slope channels of the Olbia continental slope are not connected with a subaerial drainage system. For this reason, during high-stand periods, most of the terrigenous input furnished to the deep water is thought to be mainly delivered by the interaction between southward-flowing alongshore currents and the wind-generated, semi-

permanent gyre centred offshore the Bonifacio Strait described by Artale et al. (1994).

Data and methods

The present study is based on the interpretation of data collected during the TIR-99 cruise carried out by Institute for Marine Sciences (ISMAR-CNR) of Bologna in 1999. A bathymetric survey was performed along the eastern Sardinian margin downslope from around 500 m water depth (Marani et al. 2004). The bathymetric data were acquired with a Kongsberg-Simrad EM12-120S and processed at ISMAR with in-house software developed by Ligi and Bortoluzzi (1989). Bathymetric and shaded relief maps were obtained by gridding the data with an interval of 25 m using Global Mapper software (Figs. 1, 2a). Subsurface information is furnished by a closely spaced grid of Airgun profiles, collected during the TIR-99 multibeam survey,

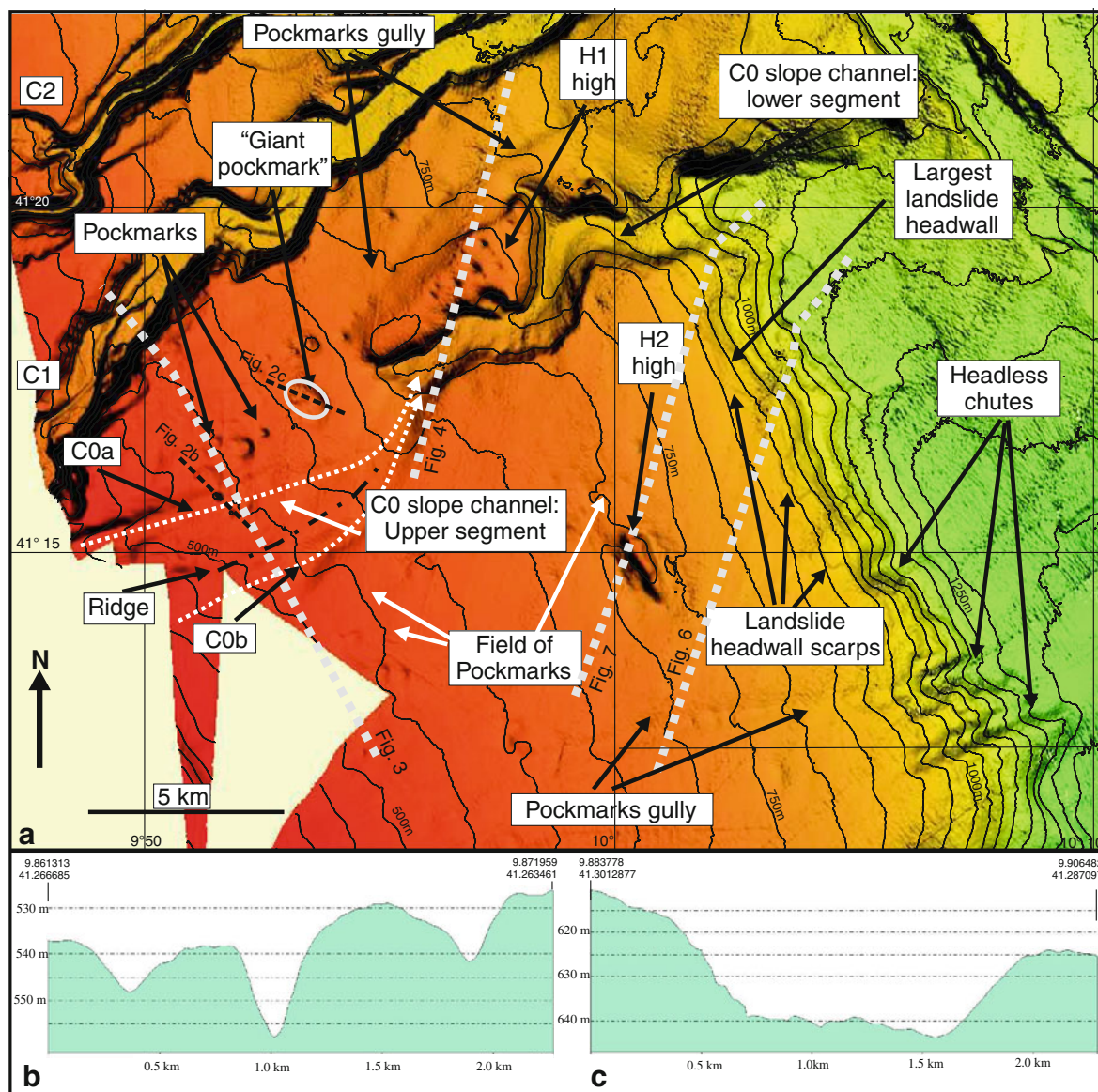


Fig. 2 Olbia continental slope: **a** shaded-relief map showing the C0 slope channel and the main fluid-venting and mass wasting related features present along the Olbia continental slope. The thin, white dotted lines indicate the course of the C0a and C0b channel forms inferred from the mapping of the corresponding linear depressions. The dashed-dotted line indicates the crest of the ridge separating the two C0a and C0b linear depressions. The black dashed lines indicate

the position of the bathymetric profiles of figure **a** and **b**. The bold dashed white lines correspond to the traces of the seismic profiles of Fig. 3 (BCO 17), Fig. 4 (TIR99-98), Fig. 6 (TIR99-101) and Fig. 7 (TIR99-100) (contour interval: 50 m); **b** bathymetric profile traced across pockmarks related to the buried sector of the C0 slope channel (see figure **a** for the location). **c** Bathymetric profile traced across the “Giant Pockmark” (see figure **a** for the location)

and by a low density grid of 30 kJ Sparker collected by ISMAR-Bologna during the BS-77 cruise in 1977.

Results

The Olbia upper continental slope: slope channels and buried channel forms

The Olbia continental slope is dissected by the C0 slope channel, which consists of an upper, completely buried

segment (from 550 to 700 m water depth) and a lower, partially buried segment (from 700 m to the base of the slope, at 1,200 m depth) (Fig. 2a). A 4 km wide, down-slope narrowing to 1 km, bathymetric low is the seafloor expression of the buried segment of the C0 channel (Fig. 2a). Within the bathymetric low, lying around 15 m below the surrounding seafloor, two subtle linear depressions (C0a and C0b) separated by a topographic high are present (Fig. 2a). The two depressions have a depth ranging from 60 to 15 m moving downslope, with a SW-NE

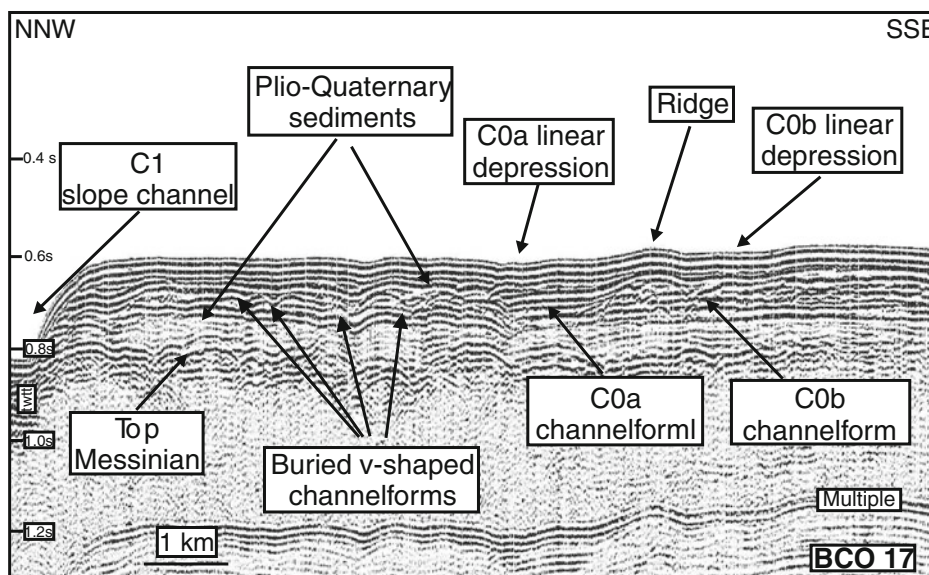


Fig. 3 NW-SE-trending 30 kJ Sparker seismic profile of the upper segment of the *C0* slope channel showing the two buried *C0a* and *C0b* channels below the subtle *C0a* and *C0b* linear depressions at the

seafloor and the further small, buried channel forms to the north (see Fig. 2 for location of the seismic line)

trend and with broad U-shaped flat floors (both channels are less than 1 km in width) (Fig. 2a). The two *C0a* and *C0b* depression converge at around 700 m depth, just upslope from the lower, partially buried sector of the *C0* channel (Fig. 2a). A seismic profile shows that the two depressions are located above two channel forms buried below around 80 ms of sediments (Fig. 3). The northern channel form, located below the *C0a* depression, is the widest, 800 m wide, with a U-shaped channel floor, filled by a package of high-amplitude, parallel reflectors (Fig. 3). The southern channel form, located below the *C0b* depression, has a gentle V-shaped profile, and is filled with more irregular reflections sometimes arranged in a cut-and fill stacking pattern (Fig. 3). To the NNW of the *C0a* and *C0b* channel forms, a series of smaller V-shaped channel forms (less than 500 m in width), filled by chaotic seismic facies, forms a ~3.5 km wide belt (Figs. 2a, 3). Similar to the *C0a* and *C0b* channel forms, the V-shaped channel forms are buried below parallel reflectors but they are not associated with seafloor linear depressions (Figs. 2a, 3).

The lower, partially buried segment of the *C0* slope channel, from around 700 m depth to the base of the slope (1,200 m water depth), is clearly evident in the bathymetric data (Fig. 2a). This segment of the *C0* channel is around 1 km wide and 100 m deep. In this segment, the *C0* slope channel is flat bottomed, and is partially infilled by parallel high-amplitude, continuous reflectors (Fig. 4). Taking into account the type of the sedimentary architectural element (channel) and the seismic facies, we can argue that the channel infill of the lower sector of the *C0* slope channel

consists of coarse-grained sediments. This sector of the *C0* channel is flanked to the north by the H1 bathymetric high (Figs. 2a, 5a).

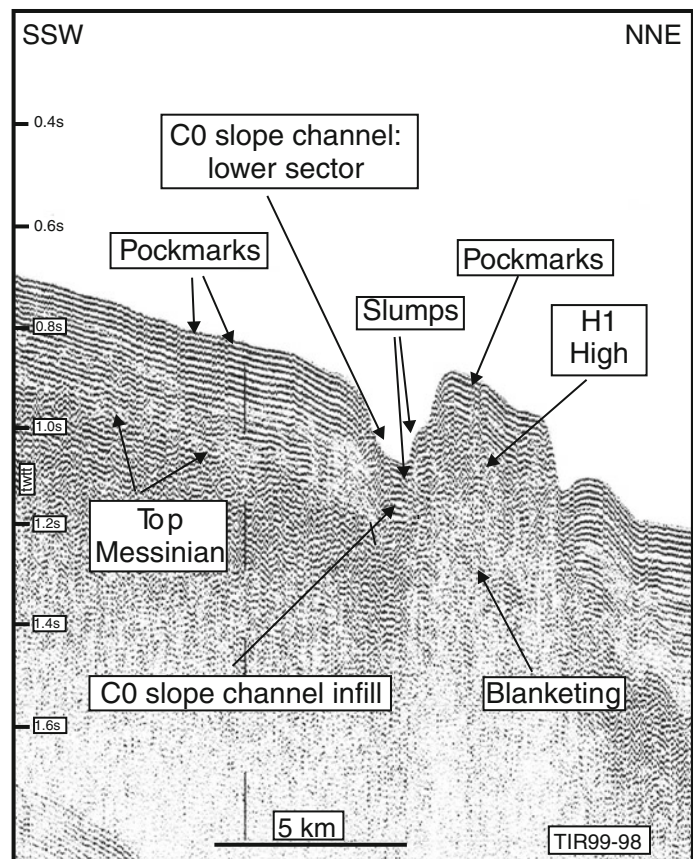
The Olbia upper continental slope: fluid-linked geomorphic features

A series of conical depressions, interpreted as pockmarks, are scattered on the seafloor of the Olbia continental slope (Figs. 2a, 5a, b). In particular, pockmarks are found both above the small V-shaped channel forms and corresponding to the *C0a* linear depression that stands above the *C0a* channel form, and more rarely in the continental slope sector south of the *C0* slope channel (Figs. 2a, 5a, b).

The pockmarks above the V-shaped channel forms can be divided into two groups: a group consisting of 8 small pockmarks (<500 m wide) that have in general a circular shape, around 20–35 m deep, with a cone-shaped profile (Fig. 2a), and an another group with at least 3 large pockmarks (up to 500 m in width) that have generally an elliptical shape, and an irregular floor (Fig. 2). In particular, the largest of these pockmarks (“Giant Pockmark” in Fig. 2a) is around 1.5 km wide, 20 m deep, and shows a subtle mounded morphology on its floor (Fig. 2a, c). Downslope from the seafloor sector above the buried V-shaped channel forms, a series of pockmarks are aligned in a single train, resembling a gully around 9 km long and 10 m deep (Figs. 2, 5a).

To the south of the *C0* slope channel, the upper Olbia continental slope is characterized by the presence of

Fig. 4 NNE-SSW-trending air gun seismic profile showing the partially buried, lower sector of the *C0* slope channel and the flanking *H1* mound. The *H1* mound is characterized by chaotic discontinuous reflections and causes the acoustic blanketing of the underlying section. The parallel, horizontal reflectors on top of the *H1* are affected by pockmarks. Slump deposits are part of the *C0* channel infill



isolated pockmarks, pockmarks clustered in fields, and pockmarks arranged in linear trains (Figs. 2a, 5b). In correspondence with the pockmarks, seismic profiles show bent reflectors that in general characterize the entire sedimentary cover (~ 0.2 s), from the acoustic basement corresponding with the top of the Messinian reflector to the seafloor (Fig. 6). However, vertical columns of bent reflectors buried below undisturbed reflectors do not reach the seafloor can be also interpreted as extinct pockmarks (Fig. 6).

Where the pockmarks are aligned, this results in a fairly straight gully similar to that developed above the buried channel forms to the north of *C0* and described previously (Fig. 2a). The gully starts at around 630 m water depth, is 15 m deeper than the surrounding seafloor, and runs along the dip of the continental slope (Fig. 2a). In the lower slope sector, at around 900 m water depth, the gully evolves in a straight, 80 m deep chute that ends at the base of the slope at 1,200 m water depth (Fig. 2a).

Two bathymetric highs, *H1* and *H2*, are also present in the Olbia continental slope (Figs. 2a, 5a, b). *H1* flanks to the north the partially buried sector of the *C0* slope channel (Figs. 2a, 5a). It has a flat top around 60 m above the surrounding seafloor and is about 5 km long and 2 km

wide, with steep flanks (12° for the flank facing the *C0* channel) (Figs. 2a, 5). The top of the *H1* high is capped by a sedimentary cover around 0.1 s thick, where pockmarks are developed (Figs. 2a, 4, 5a). The pockmarks above the *H1* high are less than 500 m in width, and around 15 m deep (Figs. 2a, 5a). Internally, the *H1* high consists of irregular to chaotic reflection, and causes the complete blanketing of the underlying units (Fig. 4). The *H1* high is not bounded by faults, and rather a moat is developed on its northern flank (Figs. 4, 5a). Given this evidence, *H1* high can be interpreted in two ways: as an erosional remnant, or as a constructional edifice consisting of hard rocks. The first hypothesis implies that the erosion of about 80 ms of sediment had occurred in the whole of the Olbia slope away from the *H1* high, and thus is quite unrealistic. For this reason, the *H1* high is best interpreted as a constructional edifice, and it can be tentatively referred to as a carbonate mud-mound. This interpretation is supported by the presence of pockmarks on the top of the *H1* high.

The *H2* high has an elliptical shape and stands in the middle slope sector (Figs. 2a, 5b). It is around 2.5 km long, with its top at about 60 m above the surrounding seafloor; it is surrounded by a circular moat (Fig. 5b). Internally it consists of strongly disturbed reflectors and the acoustic

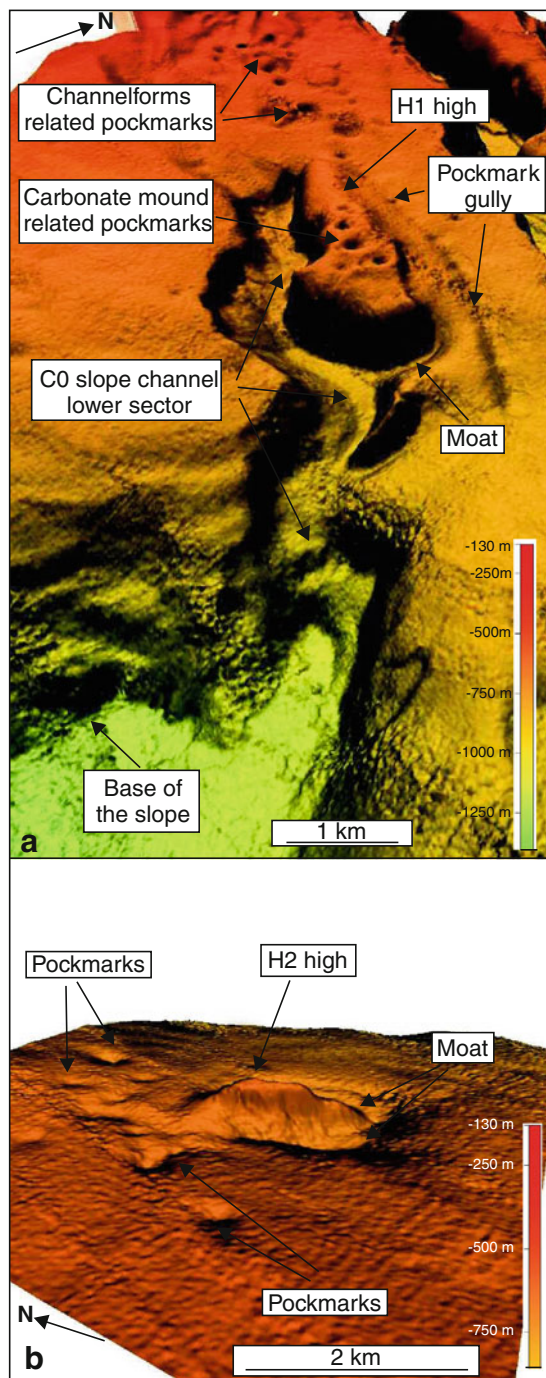


Fig. 5 3D perspective views of the fluid-venting-related features of the Olbia continental slope. **a** Particular of the *C0* slope channel and of the flanking *H1* high and of the pockmarks related to these geomorphic elements. The gully formed as a consequence of linear coalescence of pockmarks is also indicated. **b** Detail of the *H2* high and of the surrounding seafloor where scattered pockmarks are present. Vertical exaggeration of $\times 7$

basement below the structure is less reflective than in the adjacent areas (Fig. 7). Given all this evidence, and its similarity with the *H1* mound, the *H2* is also interpreted as a hard rock, constructional edifice.

The Olbia lower continental slope: mass wasting processes

The lower sector of the Olbia continental slope, between 800 and 1,200 m water depth, has an average dip of 6° , and this setting is likely to be controlled by the presence of the main extensional fault that separates the Olbia slope from the Olbia basin plain. This sector is the only sector of the Olbia continental slope that is affected by mass wasting processes: a network of various linear or arcuate escarpments arranged in a stepwise pattern, mark the beginning of the lower slope sector (Fig. 2a). The headwall scars cover a total area of around 8 km^2 (totalling about 40% of the total lower slope area). The largest headwall scars are located just southward from the lower reach of the *C0* slope channel. They are arcuate, 1.3 km wide, with the evacuation area set at around 40 m below the undisturbed, surrounding seafloor (Fig. 2a).

The rotated blocks underwent only very limited down-slope translation and are found perched above the base of slope as displaced masses (Figs. 2a, 8). Slumping and other mass movement processes are presumably recent, as revealed by truncated surficial reflectors, which can be an indicator that instability is still in progress (Figs. 6, 7).

Upslope from the rotated blocks, at 900 m depth, two landslide scars, around 1.5 km wide, with a relief of around 20 m, nucleate in correspondence with the break in slope that marks the edge of the high-gradient sector (6°) of the continental slope (Figs. 2a, 8). To the south of the landslide scars, a subdued escarpment can correspond with an area of incipient failure (Fig. 3). The landslides are not associated with pockmarks; the closest one is located about 3.5 km upslope from the network of headwall scars (Figs. 2a, 8).

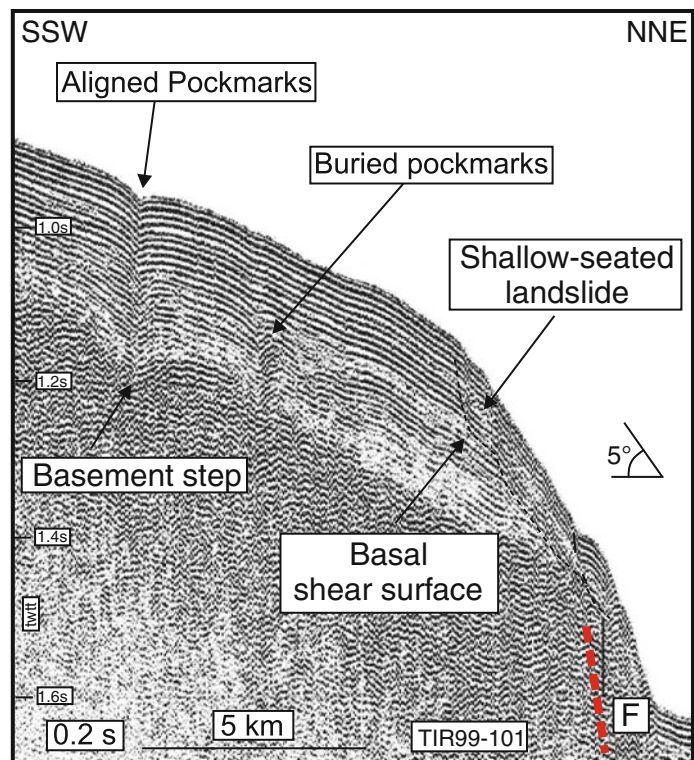
South of the landslide scars, the distal slope sector is also dissected by a series of rectilinear headless chutes (Figs. 2a, 8). One of the chutes is connected with a linear train of pockmarks on the upper slope (Fig. 2a). The chutes are linear, generally 3 km long and around 500 m wide, with a gradient of 5° – 6° . The headless chutes end at the base of the slope, where no evidence of related fan-shaped deposits is present (Figs. 2a, 8).

Discussion

Subseafloor setting as a control on the development of pockmark fields

Pockmarks are generally interpreted as the expression of upward fluid migration and seafloor seepage from over pressured biogenic/thermogenic methane, oil, or other pore fluids (Judd and Hovland 2007). In the Olbia continental slope, the presence of buried pockmarks, and pockmarks at

Fig. 6 Seismic profile crossing the southern train of linear of pockmarks. It overlies a step in the basement that likely corresponds with an inactive extensional fault. Buried pockmarks are also present. The lower, high gradient Olbia slope sector is dominated by landslide processes, with perched rotated blocks that show a very limited translation along a basal shear surface. *F* main extensional fault separating the Olbia continental slope from the Olbia basin plain



the seafloor, are evidence that upward fluid migration has been a long-lasting process, and could be active in the present. The nucleation of the observed pockmarks just above the acoustic basement, corresponding with the Messinian unconformity, indicates that the source for the ascending fluids is in the Messinian or in the deeper pre-Messinian deposits. A similar, deep source for fluids has been reported from many areas of fluid seepage in the Mediterranean areas (Baraza and Ercilla 1996; Woodside et al. 1997; Acosta et al. 2001; Casas et al. 2003; Somoza et al. 2003; Geletti et al. 2008; Gamberi and Rovere 2010).

Regarding the triggering mechanisms for pockmark development, we must take into account that the eastern Sardinian margin is tectonically inactive (Sartori 1990; Marani et al. 2004), thus earthquakes cannot be advanced as a triggering agent for fluid overpressure development and subsequent pockmark formation. Similarly, pockmarks in the OB cannot be due to gas hydrates, which are not present in the subseafloor of the study area (Klauda and Sandler 2005). Thus, with the available data, the precise cause for overpressure build up and pockmark formation in the Olbia slope cannot be determined.

The largest field of pockmarks of the Olbia slope is located in correspondence with the upper, buried sector of the C0 slope channel and in the seafloor sector above the small V-shaped channel forms to the north of it (Fig. 2a). The infill of the two branches (C0a and C0b) of the upper

sector of the C0 slope channel and of the small V-shaped channel forms to the north of it is made up of mostly discontinuous high-amplitude reflectors, which may correspond to sand-prone sediment (Fig. 3). The sandy sediments are buried below a sediment drape that was deposited after the channel activity ceased and presumably consists of fine-grained and mostly hemipelagic slope deposits that, having a thickness of around 0.1 s may act as an impermeable barrier (Fig. 3). Pockmark arrays following the course of buried channels have been observed along the west African continental margin (Haskell et al. 1997; Gay et al. 2006; Pilcher and Argent 2007). They have been interpreted as resulting from vertical fluid escape from the channel infill that, acting as a drainage pipe, entraps fluids rising from deeper levels (Gay et al. 2006). Following overpressure development, the fluids are released from the channel infill (Gay et al. 2003, 2006). A similar mechanism can explain the distribution of pockmarks above the channels in the Olbia slope that thus represents a further example showing the efficiency of subsurface lithologies in controlling fluid migration plumbing systems and the location of seafloor seepage.

The available data are not sufficient to precisely determine the setting of the gully resulting from the train of pockmarks in the southern part of the study area. However, in the available seismic line the linear array of pockmarks overlies a basement step that may be the result of a blind

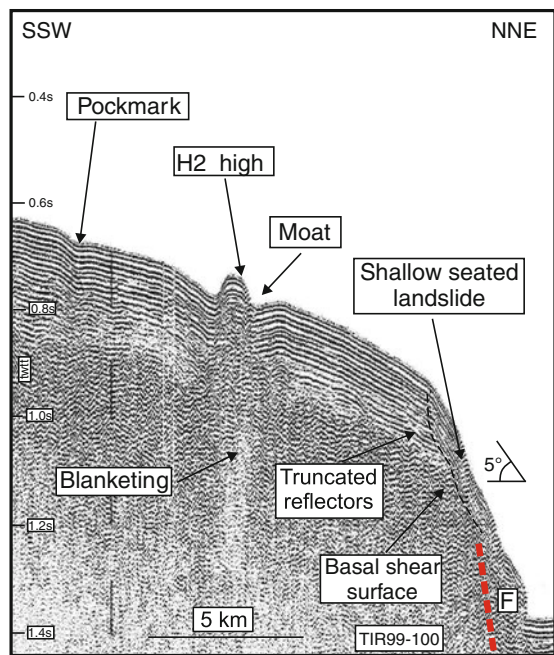
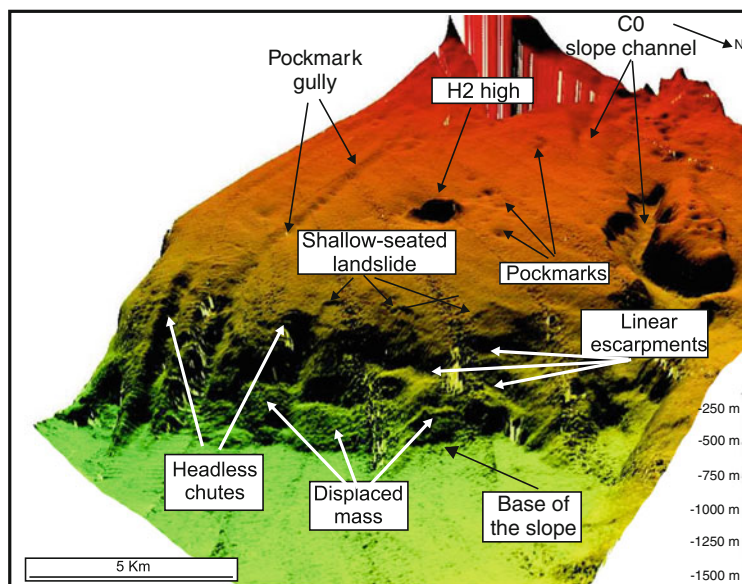


Fig. 7 N-S-trending air gun seismic profile of the middle to lower sector of the continental slope of the Olbia basin. The H2 high is characterized by chaotic reflections and causes the acoustic blanketing of the underlying section. It is flanked by a moat. It is draped by continuous reflectors that likely represent fine-grained deposits. Landslide processes are prevalent in the lower, high-gradient slope sector, and presumably are active at the present day. F main extensional fault separating the Olbia continental slope from the Olbia basin plain

fault. Therefore the gully may be the result of fluid migrating and focussing along a tectonic discontinuity. A similar case has been documented by Pinet et al. (2009) on the seafloor of the St. Lawrence Estuary, where an

Fig. 8 3D perspective view of the investigated sector of the Olbia continental slope. The complex network of linear landslide scars with linked deposits are evident in the lower slope sector. At the break in slope that marks the passage between the lower slope and the more gentle upper slope, a series of km-wide shallow-seated landslide scars are present. No geomorphic features related to seafloor instability are evident in the upper Olbia continental slope, which is dominated by features linked with fluid flow focusing. Vertical exaggeration of $\times 8$



alignment of pockmarks is structurally controlled by the buried basement.

Fluid seepage and carbonate mounds

In the Olbia continental slope, clusters of randomly distributed pockmarks are also found away from the buried channels (Fig. 2a). Clusters of pockmarks are found in association with the topographic highs along the slope: one of the clusters is located around the H2 high, and pockmarks are also found on the top of the H1 high (Fig. 5a, b). Although precise age relationships between the pockmarks and the growth of the H1 high, which is interpreted as a carbonate mud mound, cannot be established, the associations of fluid venting features with carbonate mounds may point to a possible linkage of seafloor seepage and mound growth. The connection between deep-water carbonate mounds and active hydrocarbon leakage has been proposed with a conceptual model by Henriot et al. (1998, 2002). In addition, the results of numerical modelling by Naeth et al. (2005) indicate that, in some cases, carbonate mounds may be surface expressions of underlying fluid migration systems. In active seepage sites, expulsion of gas-rich fluids commonly supports the precipitation of chemosynthetic-derived, authigenic carbonates as crust or concretion at the sediment/water interface (Judd and Hovland 2007). Hydrocarbon-derived, vent-related carbonate hard-grounds or build-ups, with their stable substrate, can be used by coral to settle and grow (Judd and Hovland 2007). The close association between deep-water carbonate ridges and structures indicative of subsurface fluid flow and seafloor seepage has been reported from many continental margins both from high-latitude settings (Hovland et al. 1994;

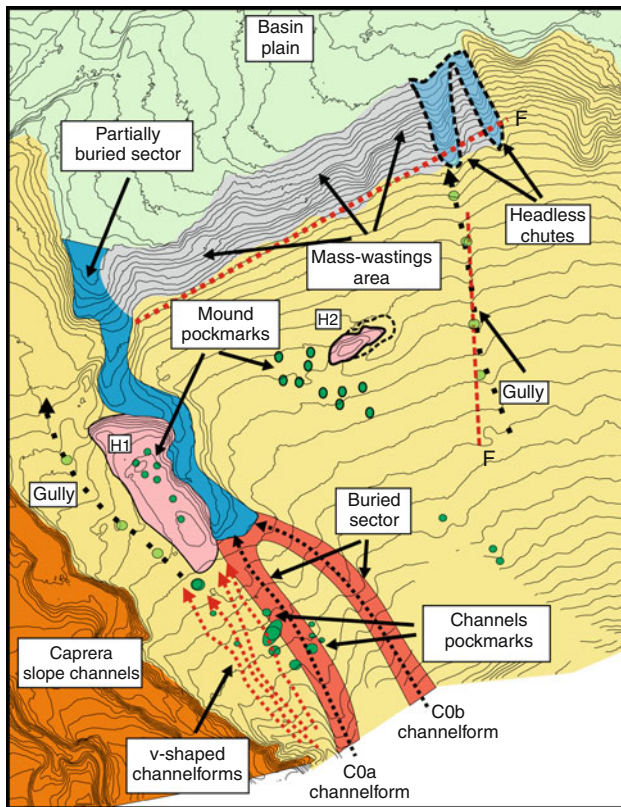


Fig. 9 Sketch showing the main sedimentary architectural elements and the main tectonic features of the Olbia continental slope and their relationships with the geomorphic features linked to fluid venting and mass wasting. *F* fault

Henriet and Mienert 1998; Masson et al. 2003; Halliday et al. 2008; Kenyon et al. 2003) and from mid-latitude, Mediterranean regions and adjacent domains (Ballesteros et al. 2008; Bayon et al. 2009a, b; Pinheiro et al. 2006, Fernández-Puga et al. 2007; Dupré et al. 2010).

No reported evidence of hydrocarbon-related plumbing systems along the seafloor and the presence of authigenic chemosynthetic carbonates are available for the eastern Sardinian margin. Therefore, the geomorphic features related to fluid venting described in this paper represent the first documentation showing that, at least in the Olbia continental slope, the escape of hydrocarbon-rich fluids that has promoted also carbonate-mound formation has been active in the past, and could also be active at the present day.

The H1 and H2 highs are at present buried beneath a thick sediment drape, thus an environmental change leading to unfavourable conditions for mound growth must have occurred in the area (Henriet et al. 2002). Based exclusively on multibeam and seismic data we can only speculate about the controls on mound growth and demise. During low-stand periods it can be argued that strong bottom currents established hydrodynamic conditions favourable for the colonisation of suitable methane-derived substrates by coral communities, with the main clastic

input funnelled within the Caprera slope channel system by the major Sardinian rivers. In high-stand periods, the bottom currents can play a minor role, owing to their less energetic activity, and the sediment-charged, river-linked nepheloid layers were able to spread unconfined across the whole Olbia continental slope, causing the mounds to stop growing and to be buried beneath thick hemipelagic deposits. Similar models for the evolution of carbonate mounds taking into account also the effects of bottom current activity has been also proposed for the carbonate mound regions in Northeast Atlantic regions such as the Norwegian margin, the Porcupine Bank and Porcupine Sea Bight, and the Rockall Trough, by O'Reilly et al. (2003), Wheeler et al. (2005), Mienis et al. (2006), White (2007), and White et al. (2007).

Mass wasting

The lower sector of the Olbia continental slope is the locus of intense mass wasting processes as the network of shallow-seated landslide scars and the presence of displaced masses at the toe of the continental slope demonstrates (Figs. 2a, 8). The slid masses appear to have rotated along a shallow basal shear surface with very limited, if any, translation, and are perched along the dip of the slope, arranged in a stepwise fashion (Figs. 6, 7, 8). The style of the failure is presumably retrogressive, with the upslope limit of the large landslides coinciding with the transition between the lower slope and the upper, gentler slope. In the Olbia continental slope, pockmarks are located in an undisturbed slope portion upslope from a network of landslides that occur in the distal, steeper slope sector, pointing to a major role of seafloor gradient in promoting sediment failure. However, fields of pockmarks located upslope from areas affected by mass wasting processes have been frequently reported in many continental slopes elsewhere, suggesting also the studied case that a close relationship between fluid-charged sediments and the lower slope landslides cannot be discounted. In addition, despite the presence of the basin master fault just below the basal shear surface of many landslides, we reject the hypothesis of a genetic linkage between this tectonic structure and mass wasting phenomena. This is supported by the lack of large historical earthquakes in the area, and by the tectonic quiescence of the whole upper sector of the eastern Sardinian margin since the Late Pliocene (Trincardi and Zitellini 1987; Mascle and Rehault 1990; Sartori 1990).

Conclusions

The present paper demonstrates that through the coupling of multibeam and seismic data it is possible to infer the

presence of several geological processes that can represent remarkable geohazards for human activities and for the environment. However, these methods do not allow us to establish whether the processes of fluid venting or mass failure are still active. In order to complete a geohazard assessment, the use of other methods that can furnish geotechnical and geochemical information regarding the state of the sediment (shear strength, pore pressure, etc.) is necessary.

This study shows that also in a passive margin not presently affected by tectonic activity, earthquakes, and gravity tectonics, and characterized by a very low sedimentation rate, relevant phenomena of subsurface fluid migration and pockmark formation can occur (Fig. 9). In particular, the pockmarks of the Olbia continental slope are the first report of subsurface fluid flow and seafloor seepage on the whole eastern Sardinian margin.

The location of pockmarks above abandoned channels and a blind fault indicates that both the stratigraphy and the structure of the subseafloor control the development of subsurface plumbing systems. In particular, the distribution of the lithologies in the subsurface can control the sites of seafloor venting. In addition, seafloor highs associated with pockmark fields point to a possible linkage between carbonate mound formation and subsurface fluid flow. The carbonate mound growth and demise have been tentatively linked to changes in the depositional regime, possibly driven by glacially-induced variations in bottom-current activity. In term of geohazard assessment both the pockmarks and the carbonate mounds represent a risk for offshore installations as submarine cables and oil pipelines. In particular, the presence of a hard substrate linked to the presence of carbonate mounds represents an additional risk for drilling operations related to exploration wells and oil rig installation and anchorage.

The lower, steeper sector of the continental slope is affected by mass wasting. Slope gradient could play a key role in controlling seafloor instability; however, the possibility that in the Olbia lower slope, rising fluid can cause overpressure and weakening of some stratigraphic horizons cannot be ruled out.

References

- Acosta J, Munoz A, Herranz P, Palomo C, Ballesteros M, Vaquero M, Uchupi E (2001) Pockmarks in the Ibiza Channel and western end of the Balearic Promontory (western Mediterranean) revealed by multibeam mapping. *Geo Mar Lett* 21:123–130
- Aloisi A, Croker P, Tizzard L, Voisey C (2000) Extensive methane-derived authigenic carbonates in the Irish Sea. *Geo Mar Lett* 27:259–267
- Andersen KJ, Huuse M (2011) ‘Bulls-eye’ pockmarks and polygonal faulting in the Lower Congo Basin: relative timing and implications for fluid expulsion during shallow burial. *Mar Geol* 279:111–127
- Artale V, Astraldi M, Buffoni G, Gasparini GP (1994) Seasonal variability of gyre-scale circulation in the northern Tyrrhenian Sea. *J Geophys Res* 99:14127–14137
- Ballesteros M, Rivera J, Munoz A, Munoz-Martín A, Acosta J, Carbo A, Uchupid E (2008) Alboran Basin, southern Spain—part II: neogene tectonic implications for the orogenic float model. *Mar Petr Geol* 25:75–101
- Baraza J, Ercilla G (1996) Gas-charged sediments and large pockmark-like features on the Gulf of Cadiz (SW Spain). *Mar Petrol Geol* 13:253–261
- Bayon GM, Loncke L, Duprè S, Caprais JC, Ducassou E, Duperron S, Etoubleau J, Foucher JP, Fuquet Y, Gontharet S, Henderson GM, Huguen C, Klauke I, Mascle J, Migeon S, Olu-Le Roy K, Ondreas H, Pierre C, Sibuet M, Stadnitskaia A, Woodside J (2009a) Multi-disciplinary investigation of fluid seepage on an unstable margin: the case of the central Nile deep sea fan. *Mar Geol* 261:92–104
- Bayon G, Henderson GM, Bohn M (2009b) U–Th stratigraphy of a cold seep carbonate crust. *Chem Geol* 260:47–56
- Berndt C (2005) Focused fluid flow on continental margins. *Philos Trans R Soc Ser A* 363:2855–2871
- Boe LR, Ottesen D (1998) Elongate depressions on the southern slope of the Norwegian trench (Skagerrak): morphology and evolution. *Mar Geol* 146:191–203
- Casas D, Ercilla G, Baraza J (2003) Acoustic evidences of gas in the continental slope sediments of the Gula of Cadiz (E Atlantic). In: Woodside JM, Garrison RE, Moore JC, Kvenvolden KA (eds) Proceedings of 7th international conference gas in marine sediments, 7–12 Oct 2002, Baku, Azerbaijan. *Geo Mar Lett*, vol 23, pp 300–310
- Cathles LM, Zheng S, Chen D (2010) The physics of gas chimney and pockmark formation, with implications for assessment of seafloor hazards and gas sequestration. *Mar Petr Geol* 27:82–91
- Cochonat P, Cadet JP, Lallemand SJ, Mazzoti S, Nouzé H, Fouchet C, Foucher JP (2002) Slope instabilities and gravity processes in fluid migration and tectonically active environment in the eastern Nankai accretionary wedge (KAIKO-Tokai’96 cruise). *Mar Geol* 187:193–202
- Dalla Valle G, Gamberi F (2010) Erosional sculpting of the Caprera confined deep-sea fan as a result of distal basin-spilling processes (eastern Sardinian margin, Tyrrhenian Sea). *Mar Geol* 268:55–66
- Dugan B, Flemings PB (2000) Overpressure and fluid flow in the New Jersey continental slope: implications for slope failure and cold seeps. *Science* 289:288–291
- Duprè S, Woodside J, Foucher JP, de Lange G, Mascle J, Boetius A, Mastalerz V et al (2007) Seafloor geological studies above active gas chimneys off Egypt (Central Nile Deep Sea Fan). *Deep Sea Res Part I Ocean Res Pap* 54:1146–1172
- Duprè S, Woodside J, Klauke I, Mascle J, Foucher JP (2010) Widespread active seepage activity on the Nile Deep Sea Fan (offshore Egypt) revealed by high-definition geophysical imagery. *Mar Geol* 275:1–19
- Fabbri A, Curzi P (1979) The Messinian of the Tyrrhenian Sea: seismic evidence and dynamic implications. *Giornale di Geologia* 43:215–248
- Fernández-Puga MC, Vázquez JT, Somoza L, Díaz del Río V, Medialdea TM, León R (2007) Gas-related morphologies and diapirism in the Gulf of Cádiz. *Geo Mar Lett* 30:231–247
- Flint SS, Hodgson DM (2005) Submarine slope systems: processes and products. *Geol Soc Lond Spec Publ*, vol 244, 225 pp
- Gamberi F, Dalla Valle G (2009) The impact of margin-shaping processes on the architecture of the Sardinian and Sicilian margin submarine depositional system within the Tyrrhenian

- Sea. In: Kneller Martinsen OJ, McCaffrey W (eds) External controls on deepwater depositional systems. *Geol Soc Lond Spec Publ*, vol 92, 392 pp
- Gamberi F, Rovere M (2010) Mud diapirs, mud volcanoes and fluid flow in the rear of the Calabrian Arc Orogenic Wedge (southeastern Tyrrhenian Sea). *Basin Res* 22:452–464
- Gay A, Lopez M, Cochonat P, Sultan N, Cauquil E, Brigaud F (2003) Sinuous pockmark belt as indicator of a shallow buried turbiditic channel on the lower slope of the Congo Basin, West African Margin. In: Van Rensbergen P, Hillis RR, Maltman AJ, Morley CK (eds) Subsurface sediment mobilization. *Geol Soc Lond Spec Publ*, vol 216, pp 173–189
- Gay A, Lopez M, Cochonat P, Levaché D, Sermondadaz G, Serann M (2006) Evidences of early to late fluid migration from an upper Miocene turbiditic channel revealed by 3D seismic coupled to geochemical sampling within seafloor pockmarks, Lower Congo Basin. *Mar Petrol Geol* 23:387–399
- Gay A, Lopez M, Berndt C, Séranne M (2007) Geological controls on focused fluid flow associated with seafloor seeps in the Lower Congo Basin. *Mar Geol* 244:68–92
- Geletti R, Del Ben A, Busetti M, Ramella R, Volpi V (2008) Gas seeps linked to salt structures in the Central Adriatic Sea. *Bas Res* 20:473–487
- Géli L, Henry P, Zitter T, Dupré S, Tryon M, Çağatay MN, Mercier de Lépinay B, Le Pichon X, Şengör AMC, Görür N, Natalin B, Uçarkuş G, Özeren S, Volker D, Gasperini L, Burnard P, Bourlange S, the Marnaut Scientific Party (2008) Gas emissions and active tectonics within the submerged section of the North Anatolian Fault zone in the Sea of Marmara. *Earth Plant Sci Lett* 274:34–39
- Halliday EJ, Barrie JV, Chapman NR, Rohr KMM (2008) Structurally controlled hydrocarbon seeps on a glaciated continental margin, Hecate Strait, offshore British Columbia. *Mar Geol* 252:193–206
- Haskell N, Nissen S, Whitman D, Antrim L (1997) Structural features on the West African continental slope delineated by 3D seismic coherency: abstract. *AAPG Bull* 81:1382
- Heggland R (2005) Using gas chimneys in seal integrity analysis: a discussion based on case histories. In: Boulton P, Kaldi J (eds) Evaluating fault and caprock seals. *AAPG Hedberg series no. 2*, pp 237–245
- Henriet JP, Mienert J (1998) Gas hydrates: relevance to world margin stability and climate change. *Geol Soc Lond Spec Publ*, vol 137, 348 pp
- Henriet JP, De Mol B, Pillen S, Vanneste M, Van Rooij D, Versteeg W, Croker PF, Shannon PM, Unnithan V, Bouriak S, Chachkine P, Porcupine-Belgica Shipboard Party (1998) Gas hydrate crystals may help build reefs. *Nature* 391:648–649
- Henriet JP, Guidard S, the ODP Proposal 573 Team (2002) Carbonate mounds as a possible example for microbial activity in geological processes. In: Wefer G, Billet D, Hebbeln D, Joergensen B, van Weering TJ (eds) Ocean margin systems. Springer, Heidelberg, pp 439–455
- Hovland M (1991) Large pockmarks, gas-charged sediments and possible clay diapirs in the Skagerrak. *Mar Petrol Geol* 8:311–316
- Hovland M, Croker PF, Martin M (1994) Fault-associated seabed mounds (carbonate knolls?) off western Ireland and northwest Australia. *Mar Petrol Geol* 15:1–9
- Hovland M, Gardner JV, Judd AG (2002) The significance of pockmarks to understanding fluid flow processes and geohazards. *Geofluids* 2:127–136
- Hovland M, Svensen H, Forsberg CF, Johansen H, Fichler C, Fossa JH, Jonsson R, Rueslatten H (2005) Complex pockmarks with carbonate-ridges off mid-Norway: products of sediment degassing. *Mar Geol* 218:191–206
- Hovland M, Heggland R, De Vries MH, Tielta TJ (2010) Unit-pockmarks and their potential significance for predicting fluid flow. *Mar Petrol Geol* 27:1190–1199
- Huguén C, Foucher JP, Mascle J, Ondréas H, Thouement M, Gontharet S, Stadnitskaia A, Pierre C, Bayon G, Loncke L, Boetius A, Bouloubassi I, de Lange G, Caprais JC, Fouquet Y, Woodside J, Dupré S (2009) Menes caldera, a highly active site of brine seepage in the eastern Mediterranean sea: “in situ” observations from the Nautinil expedition (2003). *Mar Geol* 261:138–152
- Huuse M, Jackson CAL, Van Rensbergen P, Davies RJ, Flemings PB, Dixon RJ (2010) Subsurface sediment remobilization and fluid flow in sedimentary basins: an overview. *Basin Res* 22:342–360
- Judd A, Hovland M (2007) Seabed Fluid Flow, the impact on geology, biology and the marine environment. Cambridge University Press, Cambridge
- Judd A, Croker P, Tizzard L, Voisey C (2007) Extensive methane-derived authigenic carbonates in the Irish Sea. *Geo-Mar Lett* 27:259–267
- Kastens K, Mascle J (1990) The geological evolution of the Tyrrhenian Sea: an introduction to the scientific results of ODP Leg 107. *Proc ODP Sci Results* 107:3–26
- Kenyon NH, Akhmetzhanov AM, Wheeler AJ, Van Weering TCE, De Haas H, Ivanov MK (2003) Giant carbonate mud mounds in the southern Rockall Trough. *Mar Geol* 195:5–30
- King LH, MacLean M (1970) Pockmarks on the Scotian Shelf. *Geol Soc Am Bull* 81:3141–3148
- Klauda JB, Sandler SI (2005) Global distribution of methane hydrate in ocean sediment. *Energy Fuels* 19:459–470
- Kvalstad TJ, Andresen L, Forsberg CF, Bergb K, Brynab P, Wangen M (2005) The Storegga slide: evaluation of triggering sources and slide mechanics. *Mar Petrol Geol* 22:245–256
- Ligi M, Bortoluzzi G (1989) Plotmap—geophysical and geological applications of good standard quality cartographic software. *Comp Geosci* 15:519–585
- Ligtenberg JH (2005) Detection of fluid migration pathways in seismic data: implications for fault seal analysis. *Bas Res* 17: 141–153
- Locat J, Gardner JV, Lee H, Mayer L, Hyghes Clarke J, Kammerer E (1999) Using multibeam sonarsurveys for submarine landslide investigations. In: Shikoku N, Yamagami T, Jian JC (eds) Proceedings of the international symposium on slope stability engineering, Balkema, pp 127–134
- Magalhães V, Vasconcelos C, Gaspar L, Monteiro H, Pinheiro L, Ivanov M, Díaz del Río V, Somoza L (2003) Methane related authigenic carbonates, chimneys and crusts from the Gulf of Cadiz, EGS—AGU—EUG Joint Assembly. *Geophys Res Abstr* 5:12842
- Malinverno A, Ryan WBF (1986) Extension in the Tyrrhenian Sea and shortening in the Apennines as result of arc migration driven by sinking of the lithosphere. *Tectonics* 5:227–245
- Marani M, Gamberi F, Bonatti E (2004) From seafloor to deep mantle: architecture of the Tyrrhenian back arc basin. *Mem Descr Soc Geol Ita XLIV*:97–108
- Mascle J, Rehault JP (1990) A revised seismic stratigraphy of the Tyrrhenian Sea: implications for the basin evolutions. *Proc ODP Sci Results* 107:617–663
- Masson DG, Bett B, Billet DSM, Jacobs CL, Wheeler AJ, Wynn RB (2003) The origin of deep-water, coral topped mounds in the northern Rockall Trough, Northeast Atlantic. *Mar Geol* 194:159–180
- Mazzini A, Ivanov MK, Parnell J, Stadnitskaia A, Cronin BT, Poludetkin E, Mazurenk E, van Weering TCE (2004) Methane-related authigenic carbonates from the Black Sea: geochemical characterisation and relation to seeping fluids. *Mar Geol* 202:153–181

- Mienis F, van Weering T, de Haas H, de Stigter H, Huvenne V, Wheeler A (2006) Carbonate mound development at the SW Rockall Trough margin based on high resolution TOBI and seismic recording. *Mar Geol* 233:1–19
- Mosher D, Piper D (2007) Analysis of multibeam seafloor imagery of the Laurentian Fan and the 1929 Grand Banks Landslide area. In: Lykousis V, Sakellarios D, Locat, J (eds) Submarine mass movements and their consequences. *Adv Nat Technol Hazards Ser*, vol 27, pp 77–88
- Naeth J, Di Primio R, Horsfield B, Schaefer RG, Shannon PM, Bailey WR, Henriot JP (2005) Hydrocarbon seepage and carbonate mound formation: a basin modelling study from the porcupine Basin (offshore Ireland). *J Petrol Geol* 28:147–166
- Normark WR, Piper DJW, Romans BW, Covault JA, Dartnell P (2009) Submarine canyon and fan systems of the California continental borderland. In: Lee H, Normark WR (eds) Earth science in the urban ocean. *Geol Soc Am Spec Pap*, vol 454, pp 141–168
- O'Brien GW, Cowley R, Quaipe P, Morse M (2002) Characterizing hydrocarbon migration and fault-seal integrity in Australia's Timor Sea via multiple, integrated remote-sensing technologies. In: Schumacher D, LeSchack LA (eds) Surface exploration case histories: applications of geochemistry, magnetics and remote sensing. *AAPG Stud Geol*, 48 and *SEG Geophys Ref Ser* 11, pp 393–413
- O'Reilly BM, Readman PW, Shannon PM, Jacob AWB (2003) A model for the development of a carbonate mound population in the Rockall Trough based on deep-towed sidescan sonar data. *Mar Geol* 198:55–66
- Paull C, Ussler W, Hollbrok WS (2007) Assessing methane release from the colossal Storegga submarine landslide. *Geo Res Lett* 34:1–5
- Pilcher R, Argent J (2007) Mega-pockmarks and linear pockmark trains on the West African continental margin. *Mar Geol* 244:15–32
- Pinet N, Duchesne N, Lavoie D (2009) Linking a linear pockmark train with a buried Palaeozoic structure: a case study from the St. Lawrence Estuary. *Geo Mar Lett* 30:517–522
- Pinheiro LM, Ivanov M, Kenyon N, Magalhães VH, Somoza L, Gardner J, Kopf A, Van Rensbergen P, Monteiro J.H, and the Euromargins-MVSEIS team (2006) Structural control of mud volcanism and hydrocarbon-rich fluid seepage in the Gulf of Cadiz: results from the TTR-15 and other previous cruises. *CIESM workshop monograph* 29, Monaco, pp 53–58
- Posamentier HW, Kolla V (2003) Seismic geomorphology and stratigraphy of depositional elements in deep-water settings. *J Sed Res* 73:367–388
- Pratson LF, Lee HJ, Parker G, Garcia MH, Coakley BJ, Mohrig D, Locat J, Mello U, Parsons JD, Choi SU, Israel K (1996) Mass-movements on submarine slopes. *Oceanography* 9:168–172
- Rise L, Sættem J, Fanavoll S, Thorsnes T, Ottesen D, Bøe R (1999) Sea-bed pockmarks related to fluid migration from Mesozoic bedrock strata in the Skagerrak offshore Norway. *Mar Petrol Geol* 23:17–28
- Rollet N, Logan GA, Kennard JM, O'Brien PE, Jones AT, Sexton M (2006) Characterisation and correlation of active hydrocarbon seepage using geophysical data sets: an example from the tropical, carbonate Yampi Shelf, Northwest Australia. *Mar Petrol Geol* 23:145–164
- Ryan WBF, Hsü KH et al (1973) Initial reports of the deep sea drilling project, vol XIII. U.S. Government Printing Office, Washington, DC
- Sartori R (1990) The main results of ODP Leg 107 in the frame of Neogene to recent geology of 614 the peri-Tyrrhenian areas. *Proc ODP Sci Results* 107:715–730
- Somoza L, Díaz-del-Río V, León R, Ivanov M, Fernández-Puga MC, Gardner JM, Hernández-Molina FJ, Pinheiro LM, Rodero J, Lobato A, Maestro A, Vázquez JT, Medialdea T, Fernández-Salas LM (2003) Seabed morphology and hydrocarbon seepage in the Gulf of Cadiz mud volcano area: acoustic imagery, multibeam and ultrahigh resolution seismic data. *Mar Geol* 195:153–176
- Steffens GS, Shipp RC, Prather BE, Nott A, Gibson JL, Winker CD (2004) The use of near-seafloor 3D seismic data in deepwater exploration and production. In: Davies RJ et al (eds) 3D seismic technology: application to the exploration of sedimentary basins. *Geol Soc Lond Memoir*, vol 29, pp 35–43
- Sultan N, Cochonat P, Bourillet JF, Cayocca F (2001) Evaluation of the risk of marine slope instability: a pseudo-3D approach for application to large areas. *Mar Georesour Geotechnol* 19:107–133
- Trincardi F, Zitellini N (1987) The rifting of the Tyrrhenian basin. *Geo Mar Lett* 7:1–6
- Ulzega A, Lecca L, Leone F, Orru U, Scarteddu L, Sechi F, et al (1988) Carta geomorfologica della Sardegna marina e continentale, 1:500,000. P.F. Oceanografia e Fondi Marini, CNR. *Ist.Geogr.de Agostini*, Novara
- van Rensbergen P, Rabaute A, Colpaert A, Ghislain TS, Mathijs M, Bruggeman A (2007) Fluid migration and fluid seepage in the Connemara Field, Porcupine Basin interpreted from industrial 3D seismic and well data combined with high-resolution site survey data. *Int J Earth Sci* 96:185–197
- Weimer P, Slatt RM (2004) The petroleum systems of deep-water settings: SEG distinguished instructor short course notes, 488 pp
- Wheeler AJ, Kozachenko M, Beyer A, Foubert A, Huvenne VAI, Klages M, Masson DG, Olu-Le Roy K and Thiede J (2005) Sedimentary processes and carbonate mounds in the Belgica Mound province, Porcupine Seabight, NE Atlantic. In: Friewald A, Roberts JM (eds) Cold-water corals and ecosystems. 2nd international symposium on deep-sea corals, Springer, Berlin, Germany, pp 571–603
- White M (2007) Benthic dynamics at the carbonate mound regions of the Porcupine Sea Bight continental margin. *Int J Earth Sci (Geol Rundsch)* 96:1–9
- White M, Roberts M, van Weering T (2007) Do bottom-intensified diurnal tidal currents shape the alignment of carbonate mounds in the NE Atlantic? *Geo Mar Lett* 27:391–397
- Woodside JM, Ivanov MK, Limonov AF (1997) Neotectonics and fluid flow through seafloor sediments in the Eastern Mediterranean and Black Seas. Parts I and II. UNESCO IOC Tech Ser no. 48
- Xie XN, Li S, He H, Liu X (2003) Seismic evidence for fluid migration pathways from an over pressured system in the South China Sea. *Geofluids* 3:245–253
- Zakeri A (2009) Estimating drag forces on suspended and laid-on-seafloor pipelines caused by clay-rich submarine debris flow impact. In: Mosher DC, Shipp C, Moscardelli L, Chaytor JD, Baxter CDP, Lee HJ, Urgeles R (eds) Submarine mass movements and their consequences: 4th international symposium. Springer, vol 28, pp 93–103